Supplementary Information

Gas-phase CO$_2$ Electroreduction over Sn-Cu Hollow Fiber

Xiao Dong,[a] Guihua Li,[a] Wei Chen,[*a] Chang Zhu,[a] Tong Li,[a] Yanfang Song,[a] Nannan Sun [a] and Wei Wei [*a,b]

[a]. *CAS Key Laboratory of Low-Carbon Conversion Science and Engineering, Shanghai Advanced Research Institute, Chinese Academy of Sciences, Shanghai 201210, P.R. China. E-mail: chenw@sari.ac.cn; weiwei@sari.ac.cn*

[b]. *School of Physical Science and Technology, ShanghaiTech University, Shanghai 201203, P.R. China*

Table of contents

1. Experimental section

1.1 Chemicals, reagents and materials

Copper powder (99.9 %, ~1 µm particles) was purchased from Shanghai Xiangtian Nano Materials Co., Ltd. Polyetherimide resins (PEI, 99 %) were purchased from SABIC Innovative Plastics (China) Co., Ltd. $NaBH_4$ (sodium borohydride, AR), $Na_3C_6H_5O_7 \cdot 2H_2O$ (sodium citrate dihydrate, AR), $SnCl_2 \cdot 2H_2O$ (stannous chloride dihydrate, AR), N-methyl-2-pyrrolidone (NMP, AR) and NaOH (sodium hydroxide, AR) were purchased from Sinopharm Chemical Reagent Co., Ltd. Nafion® membrane (N117) was purchased from DuPont de Nemours, Inc. Prior to use, the Nafion® membrane was treated by successive immersion at 80 °C for 1 h of each following step: first in H_2O_2 in order to remove organic impurities, then in H_2SO_4 for activation, and in deionized water to remove traces of solutions. Other chemicals and reagents were used as received without further purification. Electrolyte solutions were prepared using 18.2 MΩ H_2O obtain via a Master-S30UVF water purification system from Shanghai Hitech Instruments Co., Ltd.

1.2 Catalyst preparation

Synthesis of Cu HF

The copper hollow fibers (Cu HFs) were fabricated via a phase-inversion method.[1, 2] In brief, copper powder, polyetherimide and N-methyl-2-pyrrolidinone were mixed and well dispersed by ball milling for 24 h, followed by degassing under vacuum for overnight. Then, the suspension was extruded through a spinneret directly using water as the inner and outer coagulant. After spinning,

the obtained fibers were kept in a water bath for 24 h to complete the phase separation process, followed by drying and straightening for 48 h. The fibers were then cut into 15 cm length and placed horizontally into quartz glass tubes in tube furnace for calcination. They were firstly calcined in 200 mL·min^{-1} air at 600 ^{o}C for 6 h to remove organic compounds, and then reduced in 200 mL·min^{-1} 5 vol.% H_2/Ar at 600 ^{o}C for 3 h to obtain Cu HFs.

Synthesis of Sn-Cu HF

Sn-Cu HFs were prepared via a modified wet chemistry reduction method with sodium citrate as stabilizing agent and sodium borohydride as reductive agent.[3] In a typical procedure, 0.452 g $SnCl_2 \cdot 2H_2O$, 0.8 g NaOH and 2.94 g $Na_3C_6H_5O_7 \cdot 2H_2O$ were dissolved in 200 mL ultrapure water to form solution A, while 0.189 g $NaBH_4$, and 0.2 g NaOH were dissolved into another 50 mL ultrapure water to form solution B. Under a magnetic stirring, the as-prepared Cu HFs were put into different precursor solutions with different $SnCl_2$ concentration which were diluted from solution A. Then excess amount of solution B was added dropwise into the mixture, followed by vigorously stirring at room temperature for 8 h. Then, the HFs were collected from the solution after washing with ultrapure water for three times, and dried overnight in a vacuum oven at 60 ^{o}C to obtain xSn-Cu HF samples, where x was the weight percentage of Sn component determined by inductively coupled plasma-optical emission spectroscopy (ICP-OES).

1.3 Catalyst characterization

The loading of Sn element in each sample was quantified via ICP on an Optima 8000 instrument. Scanning electron microscopy (SEM) measurements were carried out on a Zeiss Supra

55 Sapphire apparatus with an acceleration voltage of 5.0 kV. X-ray diffraction (XRD) tests were performed on a Rigaku Ultima IV X-ray diffractometer with Cu Kα radiation (λ=1.5418 Å) under 40 kV, 40 mA and a scanning speed of 8 $^{\circ}\cdot min^{-1}$. X-ray photoelectron spectra (XPS) were obtained on a Thermo Fisher Quantum 2000 Scanning ESCA Microprobe instrument with a monochromatic excitation source of Al Kα radiation (hv=1486.6 eV) performed under 12 kV and 4 mA. The binding energies in all XPS spectra were calibrated according to the C 1s peak (284.8 eV). And the XPS spectra were deconvoluted by using Thermo Avantage software after a Shirley background subtraction procedure.

1.4 Electrochemical characterization

Gas-phase CO_2 electrochemical reaction system

The gas-phase electrochemical reaction system based on hollow fiber electrode for electrochemical performance test was shown in Scheme 1. Single hollow fiber was used as the working electrode (WE) and support. Nafion® membrane was covered on the surface of hollow fiber as the solid electrolyte and diaphragm between anode and cathode. Stainless steel mesh (SSM) was then deployed on the surface of Nafion®, functioning as the counter electrode (CE). The inner and outer sides of solid electrolyte were divided as cathode and anode chambers. The inner side (cathode chamber) was fed with 2 mL·min^{-1} CO_2, and the reduction products in exhaust was tested by an on-line GC (gas chromatograph). The outer side (anode chamber) was fed with 20 mL·min^{-1} Ar. Both gases were humidified via water bubblers to maintain enough humidity of the electrolyte

membrane. The gas-phase electrochemical tests were conducted in an oven at 80 ^oC, to guarantee sufficient proton conductivity in the solid electrolyte.

Electrochemical reduction of CO_2

CO_2 electroreduction tests were conducted via the aforementioned two-electrode gas-phase electrochemical reactor. Since no liquid electrolyte was used in the reaction system, no typical reference electrode (RE) such as KCl-saturated Ag/AgCl electrode was applied either. CO_2 was delivered into the cathode compartment in a constant rate of 2 mL·min^{-1} and purged for 30 min prior to the beginning of experiments. Then the potentiostatic electrolysis was performed with a Biologic VMP3 potentiostat at each potential for 1 h. All of the applied potentials were versus counter electrode since no reference electrode was in the reaction system.

Electrochemical characterization

Electrochemically active surface area (ECSA) measurements were carried out in the potential range from -0.45 to -0.55 V vs. CE at different scan rates of 10, 20, 30, 40 and 50 mV·s^{-1} via the aforementioned Biologic VMP3 potentiostat. The electrochemical impedance spectroscopy (EIS) tests were performed at OCV, -1.2, -1.4, -1.6 and -1.8 V vs. CE in the frequency range of 1 MHz to 0.1 Hz. Prior to the experiments, the applied gas-tight electrolysis cell was purged with CO_2 for at least 30 min. During the experiments, CO_2 was continuously delivered into the cathode compartment at a constant rate of 2 mL·min^{-1}.

Gas product analysis

4

The gas products of CO_2 electroreduction measurements in the cathode compartment were detected every half hour by an online Shimadzu GC-2014 gas chromatography equipped with a Molecular sieve-13X 60/80 column, a Plot-Q80/100 column, two flame ionization detectors (FIDs) and one thermal conductivity detector (TCD). FID1 was used for testing organic oxygenate products, while FID2 was used for testing hydrocarbons and CO (converted and tested as CH_4 via a built-in methanation converter). TCD was for H_2 testing. Argon was used as the carrier gas for the online-GC. The yields (Y_i, mol·cm^{-2}·h^{-1}) and faradaic efficiencies (FE_i, %) of gas products were calculated as follows [4]:

$$Y_i = c_i F_{CO_2}/S$$

Equation (1)

$$FE_i = n_i c_i F_{CO_2} Ft/Q$$

Equation (2)

Where c_i (mol·L^{-1}) is the concentration of the reduction products in gas phase, F_{CO_2} (L·h^{-1}) is the flow rate of CO_2, S (0.5 cm^2) is the effective reaction area for the gas-phase reaction system, n_i is the number of electrons transferred to form corresponding reduction product i, F (96485 C·mol^{-1}) is the Faraday constant, t (h) is the reaction time and Q (C) is the total charge transferred during the electrochemical reaction at each potential.
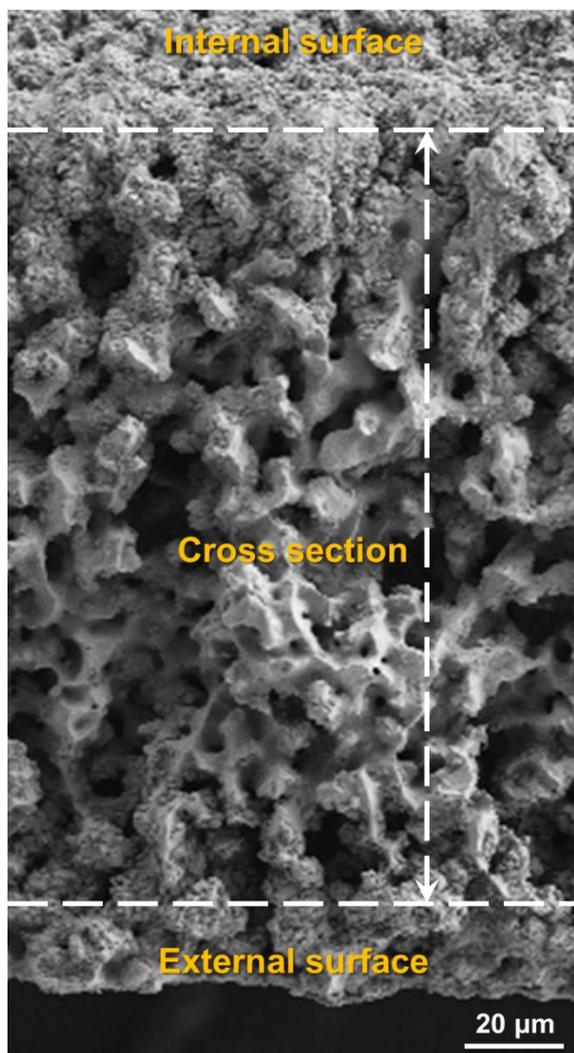
2. Supplementary figures and tables

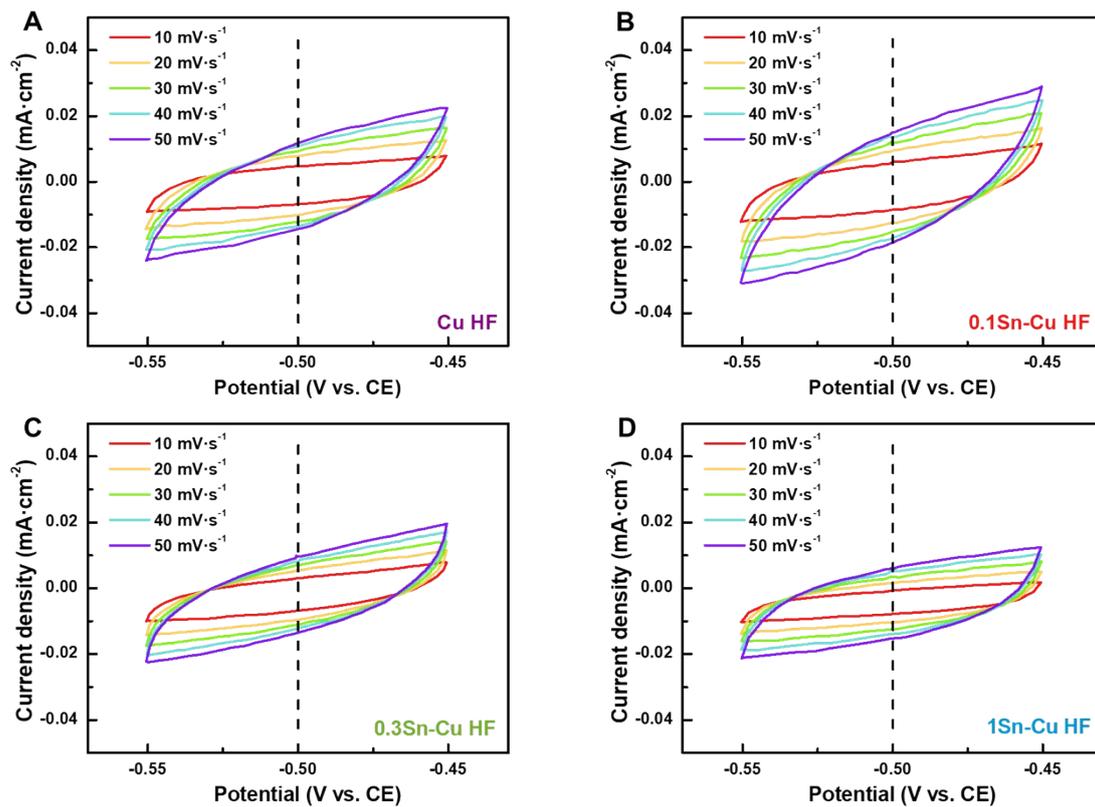**Fig. S1.** SEM image of the internal, external surfaces and cross section of 1Sn-Cu HF electrode.

Fig. S2. CV curves of (A) Cu HF, (B) 0.1Sn-Cu HF (C) 0.3Sn-Cu HF and (D) 1Sn-Cu HF in the potential range from -0.45 to -0.55 V vs. CE with different scan rates.

Table S1. External surface and average atomic Sn/Cu ratio of obtained by XPS and ICP measurements respectively.

Sample	$(Sn/Cu)_{XPS} \times 10^3$	$(Sn/Cu)_{ICP} \times 10^3$	$\dfrac{(Sn/Cu)_{XPS}}{(Sn/Cu)_{ICP}}$
0.1Sn-Cu HF	290	0.54	548
0.3Sn-Cu HF	450	1.60	282
1Sn-Cu HF	730	5.35	137

Table S2. Comparison of gas-phase CO_2 electroreduction performances on Cu-based catalysts.

Sample	Current density /mA·cm^{-2}	Potential /V	Main product i	Formation rate of i /umol·g$_{cat}^{-1}$·h^{-1}	Formation rate of i /nmol·cm^{-2}·h^{-1}	Faradaic efficiency of i /%	Testing temperature /°C	CO$_2$ flowrate /mL·min^{-1}	Relative humidity /%	Electrolyte	Counter electrode	Ref.
Cu HF	-0.11	-1.4	Acetaldehyde	/	25.3	6.0						
			Acetone	/	2.9	1.1						
0.1Sn-Cu HF	-0.23	-1.4	Acetaldehyde	/	70.1	8.2						
			Acetone	/	34.5	6.4	80	2.0	47.3	Nafion®	SSM	This work
0.3Sn-Cu HF	-0.18	-1.4	Acetaldehyde	/	64.0	9.5						
			Acetone	/	51.1	12.2						
1Sn-Cu HF	-0.13	-1.4	Acetaldehyde	/	58.3	12.0						
			Acetone	/	18.2	6.0						
	-0.3	-6.0	Methane	/	/	0.12	30		72.5			
Cu felt	-0.5	-6.0	Methane	/	/	0.08	50	100	73.3	Fumapem	Ir/Ti felt	5
	-0.8	-6.0	Methane	/	/	0.05	70		73.7			
Cu-G	1.6	-1.5	Methanol	18	9	0.09						
Cu-AC	1.6	-2.75	Acetaldehyde	110	55	0.93	90	0.5	25.0	Sterion®	IrO$_2$	6
Cu-CNF	1.6	-2.1	Acetaldehyde	20	10	0.17						
Cu-CNF	0.8	-0.5	Acetaldehyde	50	25	0.84	110	0.5	/	PBI	IrO$_2$	7
	1.6	/	Acetaldehyde	120	60	1.01						
	0.8	/	Methanol	25	12.5	0.25						
Cu	1.6	-2.1	Methanol	40	20	0.20						
	2.4	/	Methanol	50	25	0.17	90	0.5	25.0	Sterion®	IrO$_2$	8
	0.8	/	Acetaldehyde	6	3	0.10						
Cu-C	1.6	/	Acetaldehyde	8	4	0.07						
	2.4	/	Acetaldehyde	10	5	0.06						

Formation rates based on area are obtained according to formation rates based on catalyst weight and catalyst loading presented in the literatures.

3. References

1 Z. Guo, W. Chen, Y. Song, X. Dong, G. Li, W. Wei and Y. Sun, *Chinese J. Catal.*, 2020, **41**, 1067-1072.

2 W. Chen, S. Chen, T. Liang, Q. Zhang, Z. Fan, H. Yin, K. W. Huang, X. Zhang, Z. Lai and P. Sheng, *Nat. Nanotechnol.*, 2018, **13**, 345-350.

3 X. Bai, W. Chen, C. Zhao, S. Li, Y. Song, R. Ge, W. Wei and Y. Sun, *Angew. Chem. Int. Ed.*, 2017, **56**, 12219-12223.

4 D. D. Zhu, J. L. Liu and S. Z. Qiao, *Adv. Mater.*, 2016, **28**, 3423-3452.

5 S. M. A. Kriescher, K. Kugler, S. S. Hosseiny, Y. Gendel and M. Wessling, *Electrochem. Commun.*, 2015, **50**, 64-68.

6 N. Gutiérrez-Guerra, L. Moreno-López, J. C. Serrano-Ruiz, J. L. Valverde and A. de Lucas-Consuegra, *Appl. Catal. B*, 2016, **188**, 272-282.

7 N. Gutiérrez-Guerra, J. L. Valverde, A. Romero, J. C. Serrano-Ruiz and A. de Lucas-Consuegra, *Electrochem. Commun.*, 2017, **81**, 128-131.

8 N. Gutiérrez-Guerra, J. A. González, J. C. Serrano-Ruiz, E. López-Fernández, J. L. Valverde and A. de Lucas-Consuegra, *J. Energy. Chem.*, 2019, **31**, 46-53.